

Prediction of L-Methionine VCD Spectra in the Gas Phase and Water Solution

Joanna E. Rode,^{*,†} Jan Cz. Dobrowolski,^{†,‡} and Joanna Sadlej^{‡,§}

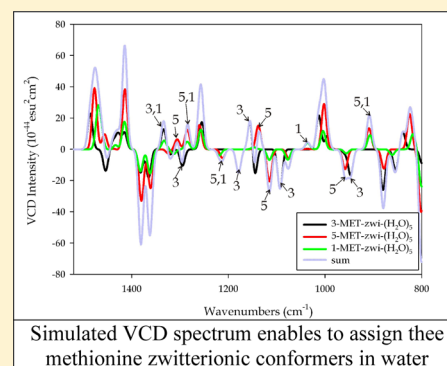
[†]Industrial Chemistry Research Institute, 8 Rydygiera Street, 01-793 Warsaw, Poland

[‡]National Medicines Institute, 30/34 Chełmska Street, 00-725 Warsaw, Poland

[§] Faculty of Chemistry, Warsaw University, 1 Pasteura Street, 02-093 Warsaw, Poland

S Supporting Information

ABSTRACT: In this paper we provide a computational study of the L-methionine conformational landscape and VCD spectra in the gas phase and a water environment simulated by implicit PCM and the hybrid model, i.e., a combination of explicit “microsolvation” and implicit models. In the gas phase, two groups of conformers differing in H-bonding, i.e., $\text{OH}\cdots\text{NH}_2$ and $\text{NH}\cdots\text{O}=\text{C}$, could be distinguished based solely on the IR $\nu(\text{OH})$ and $\nu(\text{NH})$ stretching vibrations range. On the other hand, VCD better reflected chain differences. The most stable $\text{OH}\cdots\text{NH}_2$ conformer was predicted to be easily detected, and the presence of two out of four $\text{NH}\cdots\text{O}=\text{C}$ conformers could be confirmed. Three zwitterionic methionine conformers were shown to dominate in water. Their VCD spectra, simulated within the hybrid model at the B3LYP-IEF-PCM/aug-cc-pVDZ level of theory, indicated that they could be recognized in the mixture. Use of the hybrid model is crucial for good reproduction of the hydrogen bonding pattern in the VCD spectra of methionine in water solution. However, the $1300\text{--}800\text{ cm}^{-1}$ region of the skeleton vibrations of methionine appeared to be relatively insensitive to the model of the solvent.



1. INTRODUCTION

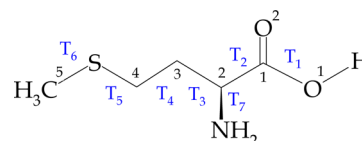
Amino acids adopt their neutral form in the gas phase and in low-temperature inert matrices, as well as in proteins and polypeptides placed in special conditions, while their zwitterionic forms dominate in water solutions. The interpretation of experimental vibrational spectroscopy data obtained for amino acids is very difficult because of the conformational variety of these molecules that complicates the prediction of their physicochemical properties. There are only very sparse reports on the vibrational spectra of amino acids in the gas phase,^{1–4} whereas the vibrational spectra of 14 amino acids (11 coded and 3 noncoded) have been registered for compounds isolated in low-temperature matrices.^{5–22} Chiroptical methods such as vibrational circular dichroism (VCD) and Raman optical activity (ROA) are useful to study configuration, conformation, and the interactions of chiral biomolecules with polar protic solvent molecules such as water.^{23–30} So far, there have been no experimental VCD measurements of amino acids taken under low-temperature matrix conditions. At the moment, the VCD matrix isolation technique is unique on the world scale.^{31–34} On the other hand, there are still no empirical rules relating the sign and magnitude of observed VCD intensities to the molecular structure, conformation, H-bonding, and solvation. Therefore, interpretation of VCD spectra relies strongly on quantum chemical calculations.

The aqueous solution is natural for biological processes; thus, most experimental studies on amino acids have been performed in water. Therefore, there is a need to develop a proper

procedure of simulations of the water environment for flexible and polar molecules such as amino acids.^{23–30,35–38} For systems in which the solute does not form hydrogen bonds with the solvent, the interpretation of VCD and ROA spectra can be performed using a reliable, modern PCM (*implicit*) approach.²⁸ However, for the adequate interpretation of systems with meaningful solute–solvent interactions, the hybrid model (a combination of *implicit* and *explicit* supermolecular approaches) is necessary.^{26–30} The same holds true for conclusive information about the conformational distributions of a solute in water.^{28,29} Studies of the VCD and ROA spectra of α -amino acids in water, the role of free amino acids in an organism, and a detailed description of their behavior in aqueous solutions have been recently reviewed.³⁹

Despite its biological importance, the vibrational spectra and conformation of L-methionine (Scheme 1) have not been

Scheme 1. L-Methionine



Received: June 3, 2013

Revised: November 5, 2013

Published: November 6, 2013

systematically studied. Together with cysteine, methionine is one of two sulfur-containing proteinogenic amino acids. Its side-chain, ending with a SCH_3 group, makes this essential amino acid highly hydrophobic, and the methionine residues of globular proteins are usually buried in the hydrophobic interior.⁴⁰ On the other hand, in methionine residues placed at the protein surface, usually clustered around an active site, the S-atom can be oxidized to a sulfoxide, protecting these sites against attack by reactive oxygen species.⁴¹

Recently, 113 conformers of neutral L-methionine have been found at the B3LYP/6-31G** level of theory.⁴² In 2002, conformation and IR spectra of seven zwitterionic L-methionine were studied at the HF/6-311++G(d,p) and B3LYP/6-31G(d) levels combined with the SCIPCM solvation model for KBr "solid solvent".⁴³ The energetic, conformational, and vibrational features of methionine zwitterion hydrated by seven water molecules were studied at the B3LYP/6-31++G* level.⁴⁴ The other IR or Raman studies referred to methionine in the crystalline phase.^{45–49}

The first VCD spectra of L-methionine in D_2O were registered in 1983 by the Nafie group.⁵⁰ The focus of the first study was on the C^*H stretching vibration VCD band of several L-amino acids in aqueous solution, including L-methionine.⁵⁰ A strong positive bias of the C^*H band was explained as originating from intramolecular hydrogen bonds between the ND_3^+ and CO_2^- groups.⁵¹

The VCD spectra of amino acids in aqueous solution in the mid-IR region are difficult to undertake because (1) water strongly absorbs in this region and therefore high concentrations and low pathlengths should be used and (2) amino acid solubilities in water at neutral pH are usually not sufficient for VCD measurements in solution. Introduction of the α -cyclodextrin (α -CD) film technique to VCD measurements in 2005⁵² allowed for the registration of the VCD spectra of several amino acids that were weakly soluble in water.^{53,54} In such measurements, for L-methionine the VCD bands have been localized at 1404, 1355, and 1328 cm^{-1} with $\Delta A/A \times 10^{-4}$ ratios equal to 1.2, -1.3 , and 1.6, respectively.^{53,54}

Quite recently, Ji et al.⁵⁵ described the VCD and IR spectra of 20 α -L-amino acids calculated at the B3LYP/cc-pVTZ level of theory. Despite the significant nonrigidity of amino acids,³⁹ the spectra were calculated based on single structures available from a structural database. Fair agreement between the calculated and experimental IR and VCD spectra was declared, and it was found that the $\rho(\text{OH})$ rocking and $\nu(\text{C}=\text{O})$ stretching modes exhibited the largest VCD rotational strengths for most amino acids.⁵⁵ The ROA spectra of methionine in water have not yet been measured.

The main purpose of this study has been to provide a platform for further interpretation of the experimental VCD and IR spectra of neutral and zwitterionic L-methionine, for which no such systematic studies have been performed. To this aim, (i) the conformational landscape of neutral and zwitterionic L-methionine in the gas phase and in water solution was characterized and (ii) L-methionine VCD and IR spectra in the gas phase and in water solution were simulated.

2. COMPUTATIONAL DETAILS

All the calculations, including geometry optimizations, harmonic/anharmonic frequencies, and IR and VCD spectra for the gas phase and water solution, were performed using the hybrid Becke three-parameter Lee–Yang–Parr density functional theory (DFT) B3LYP functional.^{56,57} The MP2

method⁵⁸ was used for population analysis because inclusion of electron correlation effects is especially important for conformational studies of flexible amino acids (cysteine,⁶ β -alanine,⁷ iso-serine,⁸ isoleucine,¹⁵ N-acetylproline,⁵ and N-acetylcysteine⁵⁹). Dunning's aug-cc-pVDZ⁶⁰ basis set was generally employed because of the size of the studied systems, yet in some cases, the aug-cc-pVTZ⁶¹ basis set was also used. The stationary structures were found by ascertaining that all the harmonic frequencies were real.

The conformational space of neutral methionine (MET) was explored through systematic rotation about the single bonds (Scheme 1) by changing the following seven dihedrals: $\text{T}_1(\text{H}-\text{O}^1-\text{C}^1-\text{C}^2)$, $\text{T}_2(\text{O}^2-\text{C}^1-\text{C}^2-\text{C}^3)$, $\text{T}_3(\text{C}^1-\text{C}^2-\text{C}^3-\text{C}^4)$, $\text{T}_4(\text{C}^2-\text{C}^3-\text{C}^4-\text{S})$, $\text{T}_5(\text{C}^3-\text{C}^4-\text{S}-\text{C}^5)$, $\text{T}_6(\text{C}^4-\text{S}-\text{C}^5-\text{H})$, and $\text{T}_7(\text{O}^2-\text{C}^1-\text{C}^2-\text{N})$. In the conformational scan 1458 structures were considered at the semiempirical AM1 level using the Spartan program.⁶² After reoptimization at the B3LYP/aug-cc-pVDZ level, 104 neutral methionine conformers were obtained. The relative abundances were calculated on both the ΔE and ΔG values relative to the most stable conformer. Methionine conformers were ordered according to decreasing population based on the ΔG values obtained at the B3LYP/aug-cc-pVDZ level ($\Delta G_{\text{B3LYP_aDZ}}(\text{X})$). Next, the 34 most stable structures according to the $\Delta G_{\text{B3LYP_aDZ}}$ values, accounting for at least 1% of conformer population, were reoptimized at the more reliable MP2/aug-cc-pVDZ level. Further discussion will be based on the $\Delta G_{\text{MP2_aDZ}}$ population results.

To account for the water solvent, two approaches were utilized. In the implicit model (IEF-PCM),^{37,38,63,64} 24 zwitterionic forms (MET-zwi) were found with B3LYP and MP2 methods combined with the aug-cc-pVDZ basis set. In the hybrid model, four to six water molecules were added to ten methionine zwitterion conformers of abundance higher than 2% at the MP2/IEF-PCM/aug-cc-pVDZ level. All the calculations were performed using the Gaussian 09 package of programs.⁶⁵

3. RESULTS AND DISCUSSION

3.1. Neutral Methionine in the Gas Phase. 3.1.1. Conformation and Energetics. The energetic data and geometrical details of neutral methionine structures are gathered in Tables 1SI–4SI and Figure 1SI in the Supporting Information. The key information is summarized in Figure 1. The following conclusions can be drawn based on energetic and structural data:

1. The energetic order of the conformers varies with the method and thermochemical correction. For example, 86-MET conformer, located at the 86th position according to the ΔG_{298} values obtained at the B3LYP level, is located at the 10th position according to the ΔG_{298} values obtained with the MP2 method and at the first position according to the MP2 total energy (Tables 1SI and 2SI of the Supporting Information.)
2. The five most stable methionine structures are the same when thermochemical corrections are taken into account, regardless of the method used (Table 3SI of the Supporting Information).
3. Neither the MP2 nor B3LYP method indicates a single dominant neutral methionine conformer in the gas phase: there are as many as seven conformers with the

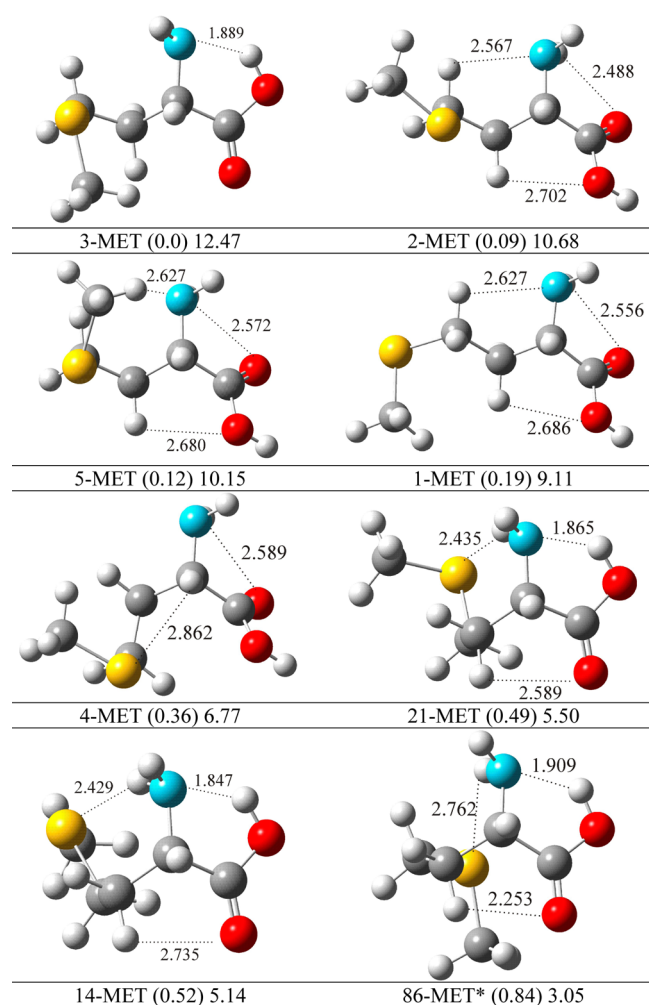


Figure 1. The MP2/aug-cc-pVDZ structures (with populations higher than 5%), relative Gibbs free energies at 298 K (in parentheses, kcal/mol), and populations (%) of the neutral methionine conformers in the gas phase. Atoms are represented as balls and are color-coded: carbon (gray), hydrogen (white), nitrogen (blue), oxygen (red), and sulfur (yellow). (*The most stable conformer according to the total energies at the $\Delta E_{\text{MP2-aDZ}}$ level.)

MP2 relative abundance higher than 5%, and the three most stable are almost equipopulated (Figure 1).

- Enlargement of the basis to aug-cc-pVTZ changes the order of conformers calculated at the DFT level. Moreover, at the B3LYP/aug-cc-pVTZ level, three conformers seem to be dominant in the mixture (Table 3SI of the Supporting Information). As for cysteine,⁶ this probably is due to an inadequate description of the S atom by the aug-cc-pVDZ basis set. However, use of the aug-cc-pVTZ basis set in the MP2 calculations or simulation of the DFT anharmonic spectra was not possible within the present project. Therefore, the presented energetic results should be treated with caution and reserve.

Because the amino acid abundances obtained at the MP2 level were shown to be more reliable than the DFT values,^{5–8,15,59} hereafter only the conformer structures populated more than 5% according to the relative MP2 Gibbs free energies are discussed. The most stable methionine conformer, *s-trans* 3-MET, populated in 12.5%, exhibits an intramolecular OH \cdots NH₂ hydrogen bond (Figure 1). The same type of intramolecular bonding has been observed for the most stable conformation of cysteine,⁶ asparagine,¹⁴ lysine,¹⁶ and β -amino acid isoserine.⁸ In the last three amino acids, the stability of the most stable conformers can be assigned to the presence of an additional H-bond with the side chain. Yet, in the 3-MET conformer, the OH \cdots NH₂ interaction seems to be the only factor stabilizing the structure.

The next four most stable conformers, which are structurally very similar, with abundances of 6.5–10.7%, are stabilized by the NH \cdots O=C intramolecular H-bond and exhibit the *s-cis* conformation of the COOH group (Figure 1). The same structural arrangements have been observed for glycine,^{12,13} α - and β -alanine,^{7,9,10,66} serine,^{18,20} valine,²¹ and isoleucine.¹⁵

The side-chain $-\text{SCH}_3$ group allows for the formation of an additional intramolecular HNH \cdots S hydrogen bond. Two intramolecular OH \cdots NH₂ and HNH \cdots S hydrogen bonds accompany the *s-trans* configuration of the COOH group in conformers 21-MET (5.5%) and 14-MET (5.1%). This specific system of two intramolecular hydrogen bonds results in a clear

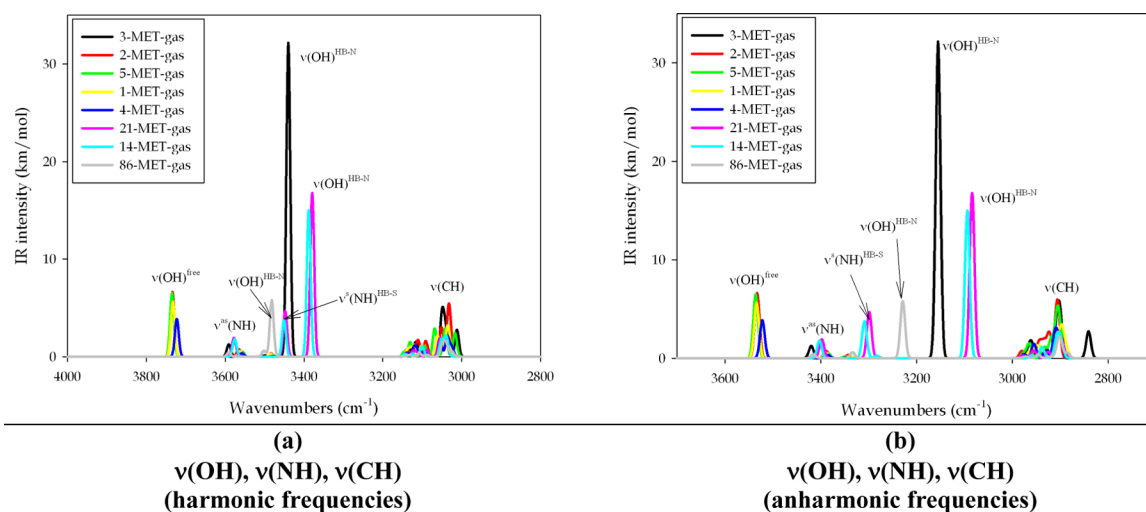


Figure 2. The Boltzmann-factors-weighted ($\Delta G_{\text{MP2/aug-cc-pVDZ}}$) harmonic (a) and anharmonic (b) IR spectra of neutral 1-methionine conformers in the most diagnostic range of the gas phase calculated at the B3LYP/aug-cc-pVDZ level.

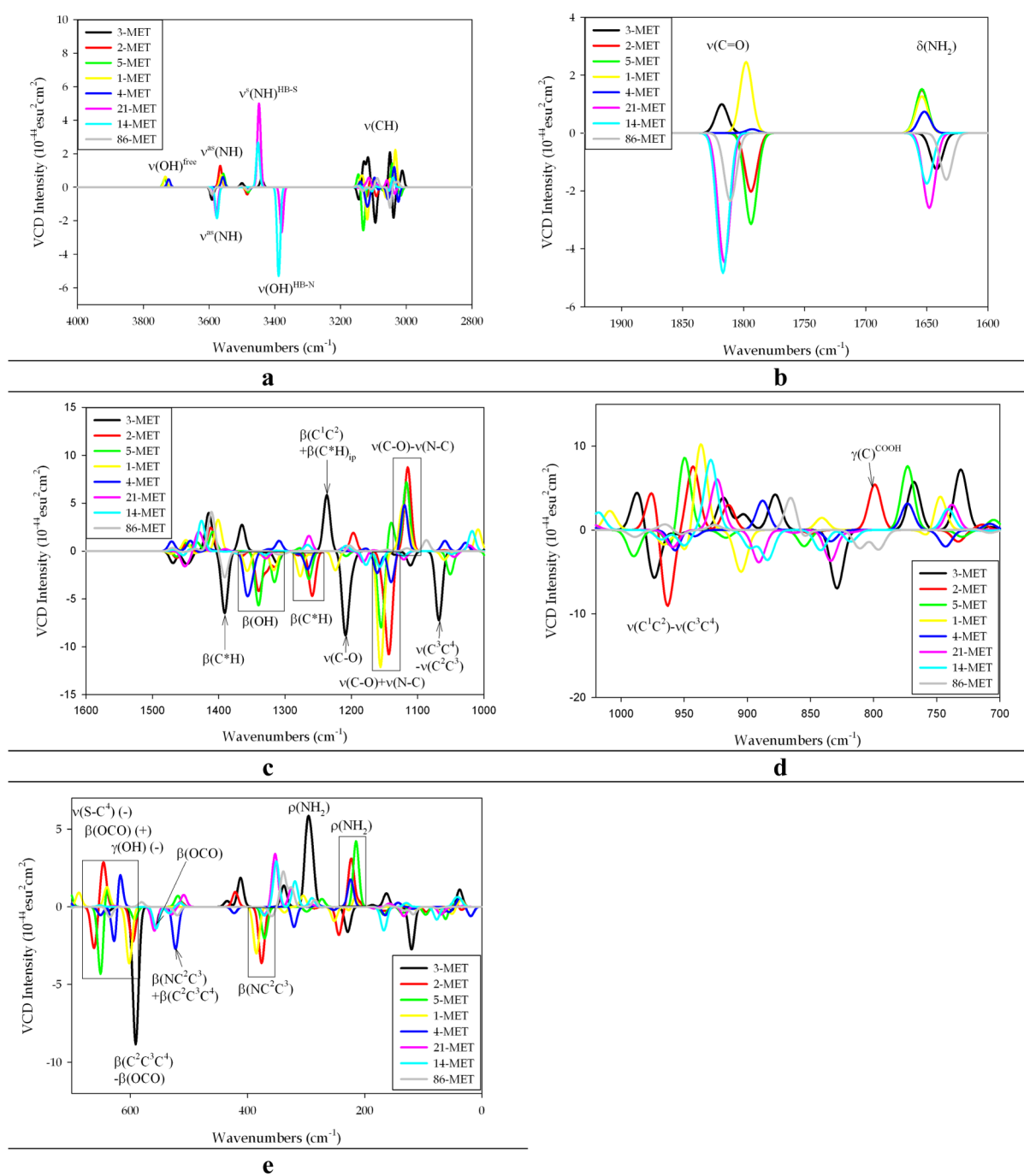


Figure 3. The Boltzmann-factors-weighted VCD spectra ($G_{\text{MP2/aug-cc-pVDZ}}$) of neutral methionine in the gas phase calculated at the B3LYP/aug-cc-pVDZ level. The bands of conformers with the $\text{NH}\cdots\text{O}=\text{C}$ intermolecular H-bond are highlighted for clarity.

manifestation of these very conformers in the IR and VCD spectra and will be discussed further.

The gas-phase infrared spectra of methionine registered at 250 °C indicated the presence of a single conformer with the free OH group and *s-cis* configuration.⁶⁷ This interpretation was based on bands characteristic for structures without intramolecular interactions with the OH group: $\nu(\text{OH})^{\text{free}}$ and $\beta(\text{COH})$ observed at 3580 and 1110 cm^{-1} , respectively. Indeed, recalculation of the neutral methionine abundances at 250 °C (at the MP2/aug-cc-pVDZ level) shows that the conformers with the $\text{NH}\cdots\text{O}=\text{C}$ intramolecular H-bond and the *s-cis* configuration of the COOH group are dominant (32.2–13.5%), while those with the $\text{OH}\cdots\text{NH}_2$ hydrogen bond

are present in negligible amounts (7.5–0.4%, Table 3SI of the Supporting Information). Summing up the above, at room temperature (25 °C), there is no dominant neutral methionine conformer and the most stable conformers exhibit $\text{OH}\cdots\text{NH}_2$ H-bonds; however, at an elevated temperature (250 °C), the structures without intramolecular OH interactions are dominant.

3.1.2. IR Spectra. Despite the fact that amino acid abundances obtained at the MP2 level are more reliable than DFT results,^{8,15,59} the latter method reproduces the experimental matrix isolation IR spectra much better than the former does.¹⁵ Therefore, the B3LYP/aug-cc-pVDZ spectra presented here for methionine conformers were weighted by population

factors obtained from the perturbation theory $\Delta G_{\text{MP2, aDZ}}(\text{X})$ terms. The calculated harmonic and anharmonic IR and VCD spectral data of the most stable neutral methionine conformers are gathered in Tables SSI–12SI of the Supporting Information.

Two kinds of H-bonds are present in the eight most stable neutral methionine structures (Figure 1), and their characteristic and selective features can be found in the ranges of stretching $\nu(\text{NH})$, $\nu(\text{OH})$, $\nu(\text{C}=\text{O})$, and $\nu(\text{C}-\text{O})$ vibrations (Figure 2 and Figure 2SI of the Supporting Information). Usually, the high-wavenumber $\nu(\text{NH})$ and $\nu(\text{OH})$ ranges are thought to be not very practical for differentiation between conformers' groups; however, we demonstrated for IR spectra of cysteine, β -alanine, and isoserine, registered in low-temperature matrices, that these ranges can be very valuable in conformer assignment and bands distanced by less than 40 cm^{-1} can be well-distinguished.^{6–8}

The following conclusions can be drawn based on the IR spectra in the 4000–2800 cm^{-1} region (Figure 2): (1) Only the presence of $\text{NH}\cdots\text{O}=\text{C}$ type conformers can be confirmed because the individual conformers of this group exhibit no characteristic spectral features. (2) Strong evidence for the presence of the $\text{OH}\cdots\text{NH}_2$ type of conformers can be obtained. The bands of 3-MET and 86-MET can be selectively found and the presence of 21-MET and 14-MET conformers can be confirmed, yet neither 21-MET nor 14-MET can be assigned as an individual species. (3) When several conformers are sparsely populated, there is still a chance to detect and assign IR bands to some of them (86-MET in this case).

A closer inspection of the methionine IR spectra below 2000 cm^{-1} enables the confirmation of the presence of groups of $\text{OH}\cdots\text{NH}_2$ and $\text{NH}\cdots\text{O}=\text{C}$ conformers rather than finding characteristic and selective bands of individual conformers (Figure 2SI of the Supporting Information). Therefore, we skip further discussion of the IR spectra.

3.1.3. VCD Spectra. The Boltzmann-factors-weighted VCD spectra calculated at the B3LYP/aug-cc-pVDZ level of the eight neutral methionine conformers are presented in Figure 3.

The 4000–2800 cm^{-1} Region. Interestingly, the conformers with the simultaneous presence of $\text{OH}\cdots\text{NH}_2$ and $\text{HNH}\cdots\text{S}$ hydrogen bonds, 21-MET and 14-MET, absorb at the same wavenumbers ca. 3578, 3450, and 3380 cm^{-1} , which are assigned to asymmetric and symmetric stretching vibrations of the NH_2 group as well stretching vibrations of the OH group, respectively (Figure 3a). Presence of the two H-bonds in 21-MET and 14-MET, instead of one in the other conformers, significantly enhanced the VCD intensities. The remaining NH and OH stretching VCD bands were weak; however, at 3730 and 3560 cm^{-1} , the $\nu(\text{OH})^{\text{free}}$ and $\nu^{\text{as}}(\text{NH})$ bands can be exclusively assigned to the conformers with free OH group. The $\nu(\text{CH})$ band range is not characteristic for conformer recognition.

The 2000–1600 cm^{-1} Region. As for the IR spectra, the VCD $\nu(\text{C}=\text{O})$ stretching bands, at ca. 1800 cm^{-1} separated by ca. 30 cm^{-1} , were grouped according to the internal hydrogen bond type (Figure 3b). However, recognition of individual conformers seems to be impossible because of bandwidth and overlapping. Similarly, the bands of $\delta(\text{NH}_2)$ scissoring mode form one complicated spectral pattern which cannot be used for assigning a particular conformer.

The 1600–1000 cm^{-1} region. For $\text{NH}\cdots\text{O}=\text{C}$ conformers, the characteristic bands were found between 1180 and 1100 cm^{-1} and at ca. 1250 and 1350 cm^{-1} (Figure 3c). The former

correspond to two groups of the $\nu(\text{C}-\text{O}) + \nu(\text{N}-\text{C})$ and $\nu(\text{C}-\text{O}) - \nu(\text{N}-\text{C})$ stretching vibration bands of opposite VCD signs, the next are assigned to $\beta(\text{C}^*\text{H})$ bending, and the latter to $\beta(\text{OH})^{\text{free}}$. Recognition of individual species based on these complex spectral patterns does not seem to be possible. On the other hand, in this very range, there are four bands specific for the most stable 3-MET conformer: $\beta(\text{C}^*\text{H})$ at 1391 cm^{-1} , $\nu(\text{C}^1\text{C}^2)$ coupled with $\beta(\text{C}^*\text{H})^{\text{ip}}$ at 1237 cm^{-1} , $\nu(\text{C}-\text{O})$ at 1209 cm^{-1} , and $\nu(\text{C}^*\text{C})$ at 1068 cm^{-1} . Importantly, in the 1600–1000 cm^{-1} region, the 3-MET conformer bands of insignificant IR intensity are intense in the VCD spectrum and *vice versa*. This shows the remarkable complementarity of the IR and VCD methods.

The 1000–700 cm^{-1} region. Strong overlapping of the bands originating from different conformers occurs in this part of the fingerprint region (Figure 3d). However, it seems that the 2-MET conformer can be identified based on a significant negative band at 964 cm^{-1} and a significant positive peak at 799 cm^{-1} , which were assigned to $\nu(\text{C}^1\text{C}^2) - \nu(\text{C}^3\text{C}^4)$ and a combination of $\delta(\text{C})^{\text{COOH}}$ deformation and $\beta(\text{C}^1\text{C}^*\text{C}^3)$ bending modes, respectively.

Although the region below 700 cm^{-1} is out-of-range for most VCD instruments, our calculations show that this region may be distinctive for the $\text{NH}\cdots\text{O}=\text{C}$ hydrogen bond conformers exhibiting a characteristic $(-)(+)(-)$ pattern between 700 and 600 cm^{-1} (Figure 3e). Additionally, for the $\text{NH}\cdots\text{O}=\text{C}$ conformers, there were specific bands at ca. 400 and ca. 200 cm^{-1} . Furthermore, it seems that the 4-MET conformer can be identified based exclusively on the band at 520 cm^{-1} , because in the entire VCD spectrum, there is no other band specific for 4-MET. Except for 3-MET, the 700–0 cm^{-1} region does not seem to be useful for the identification of the $\text{OH}\cdots\text{NH}_2$ type of conformers. For 3-MET, there are strong negative and positive bands at ca. 600 and 280 cm^{-1} , respectively.

Summing up, the results obtained for the gas phase show that identification of individual conformers based on (low-temperature matrix) IR and VCD spectra seems to be quite difficult because no conformer is dominant in the gas phase. Yet, two groups of conformers with different kinds of hydrogen bonding, $\text{OH}\cdots\text{NH}_2$ and $\text{NH}\cdots\text{O}=\text{C}$, can be unequivocally recognized. The IR spectra are very sensitive to H-bond formation, and thus this technique is an excellent tool to recognize the type of such interactions. On the basis of only the $\nu(\text{OH})$ and $\nu(\text{NH})$ stretching vibration bands, most methionine conformers with the $\text{OH}\cdots\text{NH}_2$ bond can be assigned, yet it does not seem to be possible to assign any individual $\text{NH}\cdots\text{O}=\text{C}$ conformers. On the other hand, the VCD spectra are not very sensitive to hydrogen bonding, except for the conformers stabilized by two $\text{OH}\cdots\text{NH}_2$ and $\text{NH}\cdots\text{S}-$ interactions. However, VCD better reflects the chain differences in methionine conformers. Therefore, the presence of two out of four $\text{NH}\cdots\text{O}=\text{C}$ conformers, i.e., 2-MET and 4-MET, can be confirmed. Also, the most stable 3-MET $\text{OH}\cdots\text{NH}_2$ -type conformer seems to be easily identifiable using the VCD technique. It seems that assignment of individual 5-MET and 1-MET conformers in both IR and VCD spectra is not possible in the presence of the other $\text{NH}\cdots\text{O}=\text{C}$ conformers.

3.2. Methionine in Water. **3.2.1. Conformations and Energetics.** Twenty three methionine zwitterions (MET-zwi) were found in water by a search performed at the B3LYP/IEF-PCM/aug-cc-pVDZ level using an implicit solvation model (Table 13SI and Figure 3SI of the Supporting Information). Next, they were reoptimized at the MP2/IEF-PCM/aug-cc-

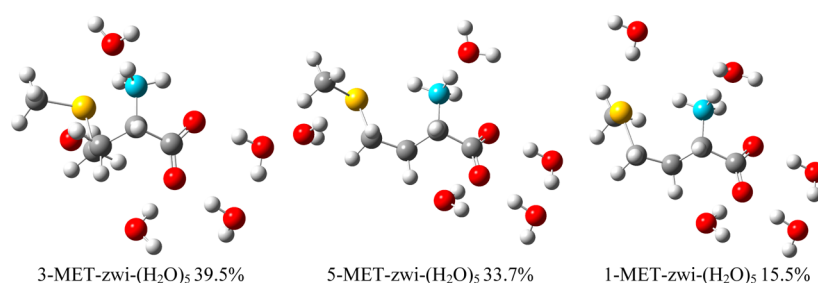


Figure 4. The B3LYP-IEF-PCM/aug-cc-pVDZ methionine-zwitterion-(H₂O)₅ complexes and abundances based on the ΔG values.

pVDZ level, and ten of them with abundance higher than 2% were used in the hybrid model for solvation. Because the PCM model yields only qualitative results, we shall not enter into a more detailed discussion of the PCM results presented in Tables 14SI–18SI of the Supporting Information.

In the hybrid model of solvation, the closest molecular surrounding is treated by the explicit presence of a few water molecules forming the first solvation sphere, while the bulk water is simulated by means of the PCM model. In this approach, it is necessary to rationally choose the number of water molecules surrounding the zwitterions. Because of computational reasons, a reasonably low number of water molecules is desired, whereas for reproduction of vibrational spectra it is important to saturate all the H-bond interaction centers. In this study, we assumed four, five, and six water molecules to be present in the first solvation sphere of the most stable methionine conformer, 3-MET-zwi. To model the hydration sphere, three steps were applied. In the first step, four water molecules were considered: three were proton-donor water molecules directed toward three free-electron pairs of oxygen atoms of the COO[−] moiety and the fourth one was either (a) a proton-acceptor engaging free H-atom of the NH₃⁺ moiety (Figure 4SIa–c of the Supporting Information), (b) a proton-donor directed toward S-atom (Figure 4SID,e of the Supporting Information), or (c) locked between the COO[−] and the NH₃⁺ groups (Figure 4SI f of the Supporting Information). Simultaneously, the favorable arrangement of three water molecules around the COO[−] group was established. In the second step, the fifth water molecule was directed to the S-atom, and thus all donor–acceptor sites of methionine were saturated (Figure 5SI of the Supporting Information). In the third step, the sixth water molecule was placed in the least favorable position between COO[−] and the NH₃⁺ moieties. The clusters with five water molecules were further analyzed as this model better reproduces the experimental IR spectra⁵⁴ as it is shown below.

The structures of the three most abundant conformers, explicitly saturated by five water molecules, exhibited two intramolecular hydrogen bonds, NH \cdots O= and NH \cdots S– (Figure 4). However, the predicted structure of solvated methionine is different from both the L-methionine zwitterions isolated in the KBr solid solvent⁴³ and the X-ray molecular structure,⁶⁸ where the presence of NH \cdots S– hydrogen bonding was either excluded or not observed. We think that this disagreement is not surprising because of significant differences in the methionine environment in crystals or crystals dispersed in KBr and in water.

Recently, Hernandez et al. investigated chain flexibility and protonation sites of methionine.⁴⁴ Three side-chain conformational angles (χ_1 , χ_2 , and χ_3) were considered for each of methionine zwitterion and are termed $g^+(60^\circ \pm 60^\circ)$, $t(180^\circ \pm$

$60^\circ)$, and $g^-(300^\circ \pm 60^\circ)$, where g and t denoted *gauche* and *trans* conformations, respectively. The distribution of the 452 optimized clusters of methionine in the presence of seven explicit water molecules was performed at the B3LYP/6-31++G* level. Energy of three conformers was greater than that of the most stable form, tg^+t , by not more than 1.17 kcal/mol. However, none of the conformers found by Hernandez et al.⁴⁴ corresponded to the most stable 3-MET-zwi-(H₂O)₅ one of $g^-g^-g^-$ arrangement found in this study. Our next conformer, 5-MET-zwi-(H₂O)₅, corresponds to the most stable tg^+t , whereas 1-MET-zwi-(H₂O)₅ and 7-MET-(H₂O)₅ to tg^+g^+ and g^-g^-t forms, respectively (Table 1).

Table 1. Comparison of the Main Dihedrals (degrees) and Energetic Data (kcal/mol) of Lowest Energy Conformers of Explicitly Hydrated L-Methionine

B3LYP-6-31++G*	χ_1	χ_2	χ_3	conformer	ΔG
Met+7H ₂ O ⁴⁴	−173,2	72,4	−175,3	tg^+t	0.0
	−52,9	−56,5	−161,5	g^-g^-t	0.62
	−77,1	72,8	−161,3	g^-g^+t	0.84
	−162,3	66,9	66,6	tg^+g^+	1.17
B3LYP/aug-cc-pVDZ	T ₃	T ₄	T ₅		
3-MET-zwi-(H ₂ O) ₅	−54,3	−71,0	−74,4	$g^-g^-g^-$	0.0
5-MET-zwi-(H ₂ O) ₅	173,3	80,0	−158,8	tg^+t	0.09
1-MET-zwi-(H ₂ O) ₅	171,1	71,6	69,3	tg^+g^+	0.48
7-MET-zwi-(H ₂ O) ₅	−60,1	−79,6	155,1	g^-g^-t	1.44

It is very important that the most stable conformer found in this study, 3-MET-zwi-(H₂O)₅, allows for good reproduction of the experimental IR spectrum of methionine in water⁵³ (Figure 5A,B). Thus both the methionine conformer and the hybrid solvent model were correctly chosen. On the contrary, the IR spectrum simulated based on PCM and the hybrid model of solvation with an additional water molecule locked between the NH₃⁺ and COO[−] groups does not fit the experimental IR spectra correctly (Figure 5C). As the simulated IR spectra of the three conformers are very similar (Figure 6SI of the Supporting Information), we do not enter into more details of the IR spectra of methionine in water.

3.2.2. The VCD Spectra of MET-zwi-(H₂O)₅ Complexes. The 3-MET-zwi-(H₂O)₅ conformer is quite different from both 5-MET-zwi-(H₂O)₅ and 1-MET-zwi-(H₂O)₅, which differed from each other by only one T₅ dihedral (Table 20SI of the Supporting Information). In consequence of the similarity of the two latter conformers, several VCD bands have contributions from both conformers, while some bands of the 3-MET-zwi-(H₂O)₅ are clearly separated from them. However, there are also some bands that can be exclusively assigned to each of the three conformers. Below, the VCD spectra in the particular regions are described in detail.

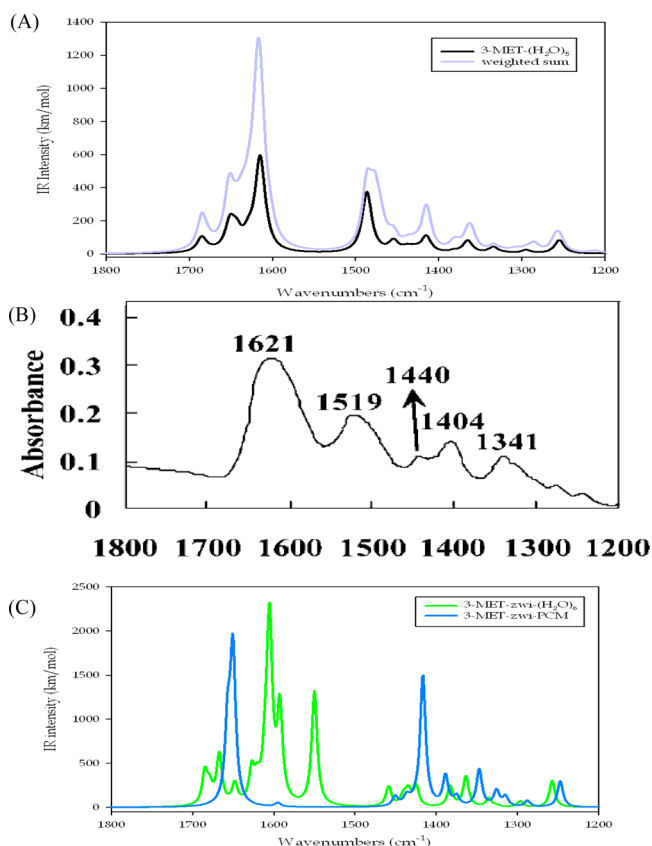


Figure 5. The absorption IR spectra of L-methionine in water: (A) the most stable conformer (black) and weighted spectrum (light blue) obtained within the hybrid-(H₂O)₅ model, (B) experimental spectrum in the α -cyclodextrin film,⁵³ and (C) the most stable conformer obtained within the PCM (blue) and hybrid-(H₂O)₆ (green) models. Reproduced from ref 53 with the kind permission of the Society of Applied Spectroscopy.

In the 4000–3000 cm⁻¹ stretching vibrations range (Figure 6a), the $\nu(\text{OH})^w$ bands (w stands for water) are positioned above, while the $\nu(\text{NH})$ and $\nu(\text{CH})$ bands are located below 3400 cm⁻¹. Despite the fact that in the three MET-zwi-(H₂O)₅ complexes the NH₃⁺ group is engaged in similar hydrogen bonding with –COO⁻, –S–, and H₂O moieties, NH stretching was very characteristic for each complex. The most characteristic VCD bands for 3-MET-zwi-(H₂O)₅ were of medium intensity (ca. $+60 \times 10^{-44}$ esu² cm²) and were associated with asymmetric and symmetric NH stretching of the NH₃⁺ group, $\nu^{\text{as}}(\text{NH}_3^+)$ at 3316 cm⁻¹ and $\nu^{\text{s}}(\text{NH}_3^+)$ at 3132 cm⁻¹. The main contribution to the $\nu^{\text{as}}(\text{NH}_3^+)$ vibration was due to the movement of the H atom H-bonded with the –COO⁻ group, while in the $\nu^{\text{s}}(\text{NH}_3^+)$ vibration, the H atom was H-bonded with water. Despite the small abundance of 1-MET-zwi-(H₂O)₅, the population-weighted VCD intensity of the band at 3268 cm⁻¹ is predicted to be significant and discriminative. It can be assigned to the $\nu(\text{NH})$ stretching of the H-atom in the NH...S interaction. On the other hand, at ca. 3250 cm⁻¹, 3-MET-zwi-(H₂O)₅ and 5-MET-zwi-(H₂O)₅ were calculated to absorb, yet with low VCD intensity: $+11$ and -12×10^{-44} esu² cm², respectively. Note that even though the 4000–3000 cm⁻¹ range is now available on commercial VCD instruments (from BioTools), the OH and NH stretching vibration VCD bands may be broad and therefore may have low diagnostic value. The $\nu(\text{CH})$ stretching VCD bands were predicted to be weak.

The most intense bands in the whole VCD spectrum were predicted to occur between 1700 and 1560 cm⁻¹ (Figure 6b). The only VCD spectrum of methionine in the range below 2000 cm⁻¹ was registered by Zhang and Polavarapu in α -cyclodextrine matrix (α -CD).^{53,54} The juxtaposition of the experimental⁵³ and calculated spectra in this paper by using different solvent simulations is presented in Figure 7. Two significant groups of bands in the range of ca. 1450–1200 and ca. 1700–1450 cm⁻¹ are predicted. The best agreement with the experimental data in the first range was obtained for the solvation model with the explicit five water molecules surrounding methionine (Figure 7A). The characteristic experimental (+)(–)(+) pattern (Figure 7B) was reproduced. The three bands predicted at ca. 1425 cm⁻¹ corresponded to the $\beta(\text{CH})$ bending vibrations of the –C⁴H₂ and C⁵H₃ groups and $\beta(\text{C}^*\text{H})$ bending vibrations coupled in-phase with the $\nu(\text{C}^1\text{–C}^2)$ stretching. Two negative VCD bands predicted at 1382 and 1356 cm⁻¹ corresponded to the $\beta(\text{C}^*\text{H})$ bendings in the plane of the C*–N bond, and the $\beta(\text{C}^*\text{H})$ bending vibrations coupled in-counter phase with the $\nu(\text{C}^1\text{–C}^2)$ stretching, respectively. The band at 1334 cm⁻¹ is the $\beta(\text{C}^*\text{H})$ bending mode in the plane perpendicular to the C*–N bond. It has to be stressed that the PCM and the hybrid model with six water molecules in the first hydration sphere did not predict the VCD spectra in this range correctly: only one band is predicted in the PCM model whereas the (–)(+), instead of (+)(–)(+), pattern is obtained using the (H₂O)₆ model (Figure 7C).

The group of bands between 1650 and 1580 cm⁻¹ corresponds to bending vibration of H₂O from the solvation sphere which overlaps with the $\nu(\text{COO}^-)$ band and several asymmetric bending vibration bands of the NH₃⁺ moiety. The band at ca. 1490 cm⁻¹ corresponds to the symmetric bending (umbrella) vibrations of the NH₃⁺ moiety. The calculated bands in the 1700 and 1560 cm⁻¹ range are predicted to be mutually overlapping, yet it seems that the 5-MET-zwi-(H₂O)₅ conformer can possibly be identified based on a shoulder band at ca. 1620 cm⁻¹ (Figure 6). Absence of the VCD bands in the experimental spectrum in the 1700–1450 cm⁻¹ range is surprising, and probably it is connected with the specific registration technique. For amino acids such as L-leucine,²⁷ L-cysteine,²⁹ and N-acetyl-L-cysteine²⁸ registered in D₂O, the $\nu(\text{COO}^-)$ VCD bands are present and are strong.

In the 1500–800 cm⁻¹ range, several significant bands of the three conformers were overlapping; however, there were some medium intensity bands which could be selectively assigned to two of the most stable methionine zwitterions. Between 1200 and 1050 cm⁻¹, the bands of 3-MET-zwi-(H₂O)₅ and 5-MET-zwi-(H₂O)₅ were well-separated and formed a characteristic (+)(+)(–)(–) spectral pattern of $\beta_1(\text{C}^*\text{H} + \text{NH})$ and $\beta_2(\text{C}^*\text{H} + \text{NH})$ vibrations (Figure 6). Although there was a medium intensity (-50×10^{-44} esu² cm²) band at 1146 cm⁻¹ for the 3-MET-zwi-(H₂O)₅, it probably will disappear in the contours of the neighboring positive bands.

It is very important that the VCD spectra in the 1300–800 cm⁻¹ range simulated using different implicit and hybrid models are, in practice, in very good harmony (see next section). This is because this range corresponds to the vibrations of the methionine zwitterion skeleton, which is relatively insensitive to environmental changes. There were, however, two exceptions: the (+)(–) pattern was observed for 3-MET-zwi-(H₂O)_{n=4,5} complexes in the 1160–1020 cm⁻¹ range, while only one positive band was predicted by the PCM model and 3-MET-zwi-(H₂O)₆ complex; bands of

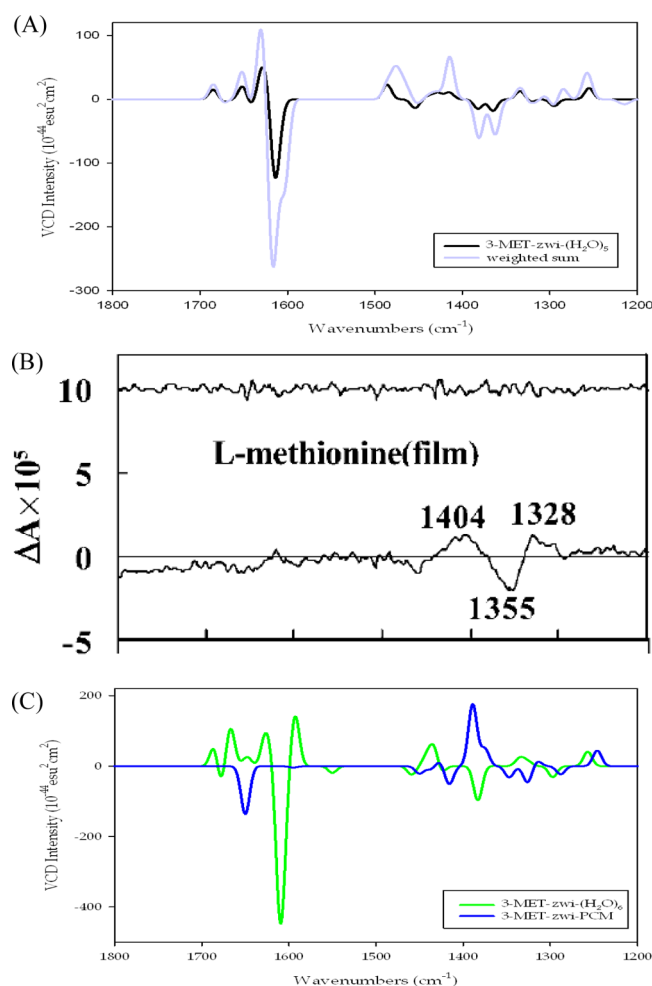


Figure 7. The VCD spectra of L-methionine in water: (A) the most stable conformer (black) and weighted spectrum (light blue) obtained within the hybrid-(H₂O)₅ model, (B) experimental spectrum in the α -cyclodextrin film,⁵³ and (C) the most stable conformer obtained within the PCM (blue) and hybrid-(H₂O)₆ (green) models. Reproduced from ref 53 with the kind permission of the Society of Applied Spectroscopy.

cm⁻¹) and +12 (3265 cm⁻¹), respectively (Figure 9). For the VCD spectra of the 3-MET-zwi-(H₂O)₄ and 3-MET-zwi-(H₂O)₅ complexes in the region sensitive to chirality transfer to

water molecules, 1700–1550 cm⁻¹, no differences were observed. On the other hand, the location of the sixth water molecule between the COO⁻ and the NH₃⁺ groups (Figure 8c) produced a remarkable change in the predicted VCD spectrum (Figure 9). The influence of the presence of the sixth water molecule on both the band position and the VCD intensities was especially striking in the 4000–3000 cm⁻¹, 1700–1550 cm⁻¹, and below 800 cm⁻¹ spectral ranges, whereas only minor changes in the 1300–800 cm⁻¹ range were observed.

On the other hand, the VCD spectra of 3-MET-zwi, except in the 1300–800 cm⁻¹ region, obtained with the PCM model alone, dramatically differed from those from the hybrid approach (Figure 9). In the 4000–3000 cm⁻¹ region of the PCM simulated spectrum, two strong VCD bands, one positive band at 3208 cm⁻¹ ($\nu(\text{NH})^{\text{IHB-S}}$; IHB-S stands for the NH \cdots S H-bond) and one negative band at 3107 cm⁻¹ ($\nu(\text{CH})$ coupled with $\nu(\text{NH})^{\text{IHB-O}}$; IHB-O stands for the NH \cdots O H-bond) were predicted. In contrast, by the hybrid approach, in the VCD spectrum of 3-MET-zwi-(H₂O)₅, all NH₃⁺ H-atoms were engaged in H-bonds contributing to positive $\nu(\text{NH})$ VCD bands.

Again, in the 1700–1500 cm⁻¹ range simulated by the PCM model alone, only one strong negative VCD $\nu(\text{C}=\text{O})$ band was predicted, whereas at least four bands of significant intensity were predicted within the framework of the hybrid model (Figure 9b). A number of bands resulted from the coupling of water bending vibrations to both symmetric and asymmetric stretching of the COO⁻ and NH groups. The intensities in the $\nu(\text{C}=\text{O})$ band region in the hybrid models were greater than those in the implicit model. The VCD spectra in the 1500–1300 cm⁻¹ range and the range below 800 cm⁻¹ were very sensitive to the solvent model used (Figure 9c,e,f).

4. CONCLUSIONS

In this paper a computational study on VCD and IR spectra of chiral methionine in the gas phase and water environment was presented. Implicit PCM and hybrid solvation models have been considered to account for the effect of hydration of methionine. The main conclusions can be summarized as follows:

1. For neutral methionine, a number of factors influences the structure and stability, but the most important is the energetic profit from the formation of the intramolecular OH \cdots NH₂ hydrogen bond and the competitive profit

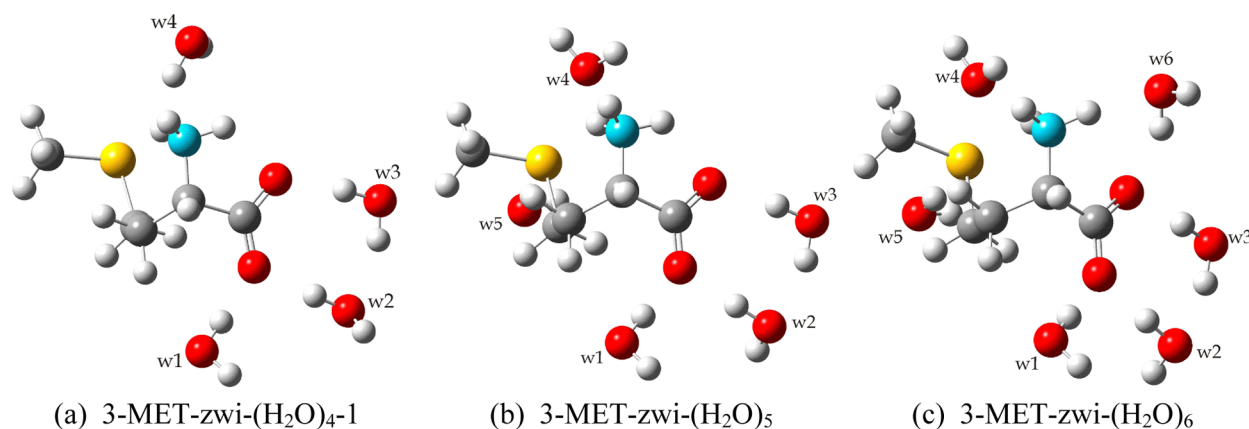


Figure 8. The B3LYP-IEF-PCM/aug-cc-pVDZ-calculated 3-MET-zwi complexes with different numbers of water molecules in the first hydration sphere in the hybrid solvation model.

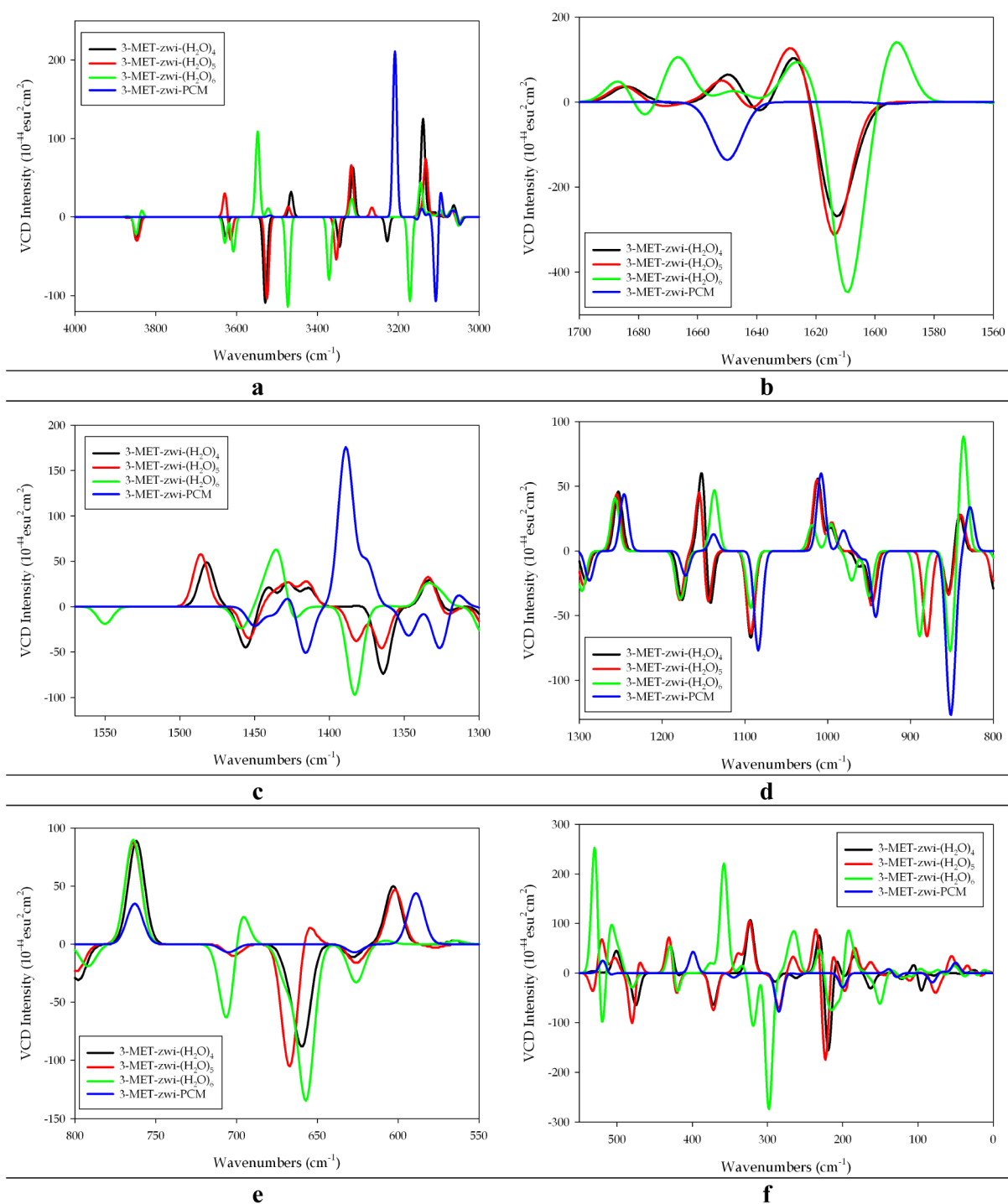


Figure 9. Influence of the solvation model on the VCD spectra of 3-MET-zwi conformer.

from adopting the *cis* configuration of the COOH group. Two groups of conformers differing in H-bonding, i.e., OH \cdots NH $_2$ and NH \cdots O=C, could be distinguished. The most stable neutral methionine conformer at 25 °C exhibits the OH \cdots NH $_2$ intramolecular hydrogen bond and the *trans* configuration of the COOH group. However, at 250 °C, conformers with the NH \cdots O=C intramolecular H-bond and *cis* COOH group configuration are dominant (32.2–13.5%), in agreement with the findings of Linder et al.,⁶⁷ while those with the OH \cdots NH $_2$ H-bond exist in negligible amounts (7.5–0.4%).

2. For the neutral methionine conformers, most individuals with OH \cdots NH $_2$ interactions could be distinguished based only on the IR ν (OH) and ν (NH) stretching vibration bands, yet the identification of individual NH \cdots O=C conformers seems to be impossible. On the other hand, hydrogen bonding interactions were not reflected in the VCD spectra, except for conformers with simultaneous OH \cdots NH $_2$ and NH \cdots S– interactions. However, VCD better reflects the chain differences, and the most stable OH \cdots NH $_2$ conformer was predicted to be easily detected; the presence of two out of four NH \cdots O=C

conformers could be confirmed. Detection of two other $\text{NH}\cdots\text{O}=\text{C}$ conformers based on the two experimental techniques does not seem to be possible.

3. The conformational landscape of zwitterionic methionine in water was explored at the B3LYP/aug-cc-pVDZ level using the PCM model. Ten zwitterions populated more than in 2% ($\Delta G_{\text{MP2-IEF-PCM}}$) were then used for hybrid model with five water molecules. On the basis of the $\Delta G_{\text{B3LYP-IEF-PCM}}$ energies, three MET-zwi-(H_2O)₅ conformers were found to be populated in ca. 40, 34, and 17%. They were stabilized by $\text{NH}\cdots\text{O}=\text{C}$ and $\text{NH}\cdots\text{S}$ intramolecular hydrogen bonds. This disagrees with findings for methionine zwitterions in crystals isolated in the KBr solid solvent⁴³ as well as the X-ray molecular structure,⁶⁸ in which the presence of $\text{NH}\cdots\text{S}$ H-bonds was excluded or not observed.
4. The calculated IR spectrum based on the most stable conformer of L-methionine in water (of 40% abundance) is in very good agreement with the experimental one.⁵⁴ Thus, both methionine conformer and the hybrid solvent model, in which all electron-donor sites have been saturated by five explicitly added water molecules, were correctly chosen. In contrast, the IR spectrum simulated by PCM and the hybrid model of solvation in which an additional water molecule was locked between the NH_3^+ and COO^- groups, did not fit the experimental IR spectra correctly.
5. The (+)(-)(+) pattern in the 1450–1300 cm^{-1} range of the experimental VCD spectrum of L-methionine in α -CD film was reproduced in the calculations based on the hybrid model. The calculated VCD spectra do not fit the experimental one in the 1700–1550 cm^{-1} range, where the chirality transfer bending vibration of H_2O from the solvation sphere coupled with the $\nu(\text{COO}^-)$ and several asymmetric bending vibrations of the NH_3^+ moiety are present. However, we think that due to some technical reasons the experimental spectrum does not contain bands in this region, because for other amino acids the $\nu(\text{COO}^-)$ VCD bands of significant intensities have been observed.
6. The VCD spectra in the ranges of 4000–1300 cm^{-1} and below 800 cm^{-1} depended strongly on the kind of solvent model used (PCM vs hybrid), including the number of water molecules in the first solvation sphere. The use of the hybrid model is crucial for accordance between simulated and experimental spectra. In the case of L-methionine, location of the sixth water molecule between the COO^- and NH_3^+ groups diminish in accordance with IR and VCD experiments. On the other hand, the 1300–800 cm^{-1} region, where the methionine zwitterion skeleton bands are mainly present, is relatively insensitive to the method of solvent treatment.
7. The VCD spectra of the three most stable MET-zwi-(H_2O)₅ complexes, calculated at the B3LYP-IEF-PCM/ aug-cc-pVDZ level, showed that NH stretching bands are very characteristic for each of the zwitterionic complexes, despite the fact that the NH_3^+ group is engaged in similar H-bonds. The remaining spectral ranges also allowed for selective assignment of two out of the three methionine zwitterions.
8. The chirality transfer bands $\beta(\text{H}_2\text{O})$ of water in the 1700–1560 cm^{-1} range are predicted to be of highest intensity in the entire VCD spectrum.

■ ASSOCIATED CONTENT

Supporting Information

The detailed energetics, geometry, structures, and frequency details of neutral methionine conformers in the gas phase and zwitterionic methionine in water and the complete author list of the Gaussian 09 package of programs. This material is available free of charge via the Internet at <http://pubs.acs.org>.

■ AUTHOR INFORMATION

Corresponding Author

*Industrial Chemistry Research Institute, 8 Rydygiera Street, 01-793 Warsaw, Poland. E-mail: joanna.rode@gmail.com. Tel: +48-22-568-24-21. Fax: +48-22-568-22-93.

Notes

The authors declare no competing financial interest.

■ ACKNOWLEDGMENTS

This research was performed within Grant N N204 443 140 funded by the National Science Center of Poland. The computational G19-4 grant from the Interdisciplinary Center of Mathematical and Computer Modeling (ICM) at Warsaw University is acknowledged for the generous allotment of computer time.

■ REFERENCES

- (1) Bakker, J. M.; Plutzer, C.; Hünig, I.; Häber, T.; Compagnon, I.; Von Helden, G.; Meijer, G.; Kleineremanns, K. Folding Structures of Isolated Peptides as Revealed by Gas-Phase Mid-Infrared Spectroscopy. *ChemPhysChem* **2005**, *6*, 120–128.
- (2) Linder, R.; Nispel, M.; Häber, T.; Kleineremanns, K. Gas-phase FT-IR-spectra of natural amino acids. *Chem. Phys. Lett.* **2005**, *409*, 260–264.
- (3) Linder, R.; Seefeld, K.; Vavra, A.; Kleineremanns, K. Gas phase infrared spectra of nonaromatic amino acids. *Chem. Phys. Lett.* **2008**, *453*, 1–6.
- (4) Hu, Y.; Bernstein, E. R. Vibrational and photoionization spectroscopy of biomolecules: Aliphatic amino acid structures. *J. Chem. Phys.* **2008**, *128*, 164311.
- (5) Boeckx, B.; Ramaekers, R.; Maes, G. The influence of the peptide bond on the conformation of amino acids: A theoretical and FT-IR matrix-isolation study of N-acetylproline. *Biophys. Chem.* **2011**, *159*, 247–256.
- (6) Dobrowolski, J. Cz.; Jamróz, M. H.; Kołos, R.; Rode, J. E.; Sadlej, J. Theoretical prediction and the first IR-matrix observation of several L-cysteine molecule conformers. *ChemPhysChem* **2007**, *8*, 1085–1094.
- (7) Dobrowolski, J. Cz.; Jamróz, M. H.; Kołos, R.; Rode, J. E.; Sadlej, J. IR low-temperature matrix and ab initio study on β -alanine conformers. *ChemPhysChem* **2008**, *9*, 2042–2051.
- (8) Dobrowolski, J. Cz.; Jamróz, M. H.; Kołos, R.; Rode, J. E.; Cyrański, M. K.; Sadlej, J. IR low-temperature matrix, X-ray and ab initio study on L-isoserine conformations. *Phys. Chem. Chem. Phys.* **2010**, *12*, 10818–10830.
- (9) Bazsó, G.; Najbauer, E. E.; Magyarfalvi, G.; Tarczay, G. Near-Infrared Laser Induced Conformational Change of Alanine in Low-Temperature Matrixes and the Tunneling Lifetime of Its Conformer VI. *J. Phys. Chem. A* **2013**, *117*, 1952–1962.
- (10) Stepanian, S. G.; Ivanov, A. Y.; Smyrnova, D. A.; Adamowicz, L. UV-induced isomerization of β -alanine isolated in argon matrices. *J. Mol. Struct.* **2012**, *1025*, 6–19.
- (11) Kaczor, A.; Reva, I. D.; Proniewicz, L. M.; Fausto, R. Importance of Entropy in the Conformational Equilibrium of Phenylalanine: A Matrix-Isolation Infrared Spectroscopy and Density Functional Theory Study. *J. Phys. Chem. A* **2006**, *110*, 2360–2370.
- (12) Bazsó, G.; Magyarfalvi, G.; Tarczay, G. Tunneling lifetime of the ttc/VIp conformer of glycine in low-temperature matrices. *J. Phys. Chem. A* **2012**, *116*, 10539–10547.

- (13) Espinoza, C.; Szczepanski, J.; Vala, M.; Polfer, N. C. Glycine and Its Hydrated Complexes: A Matrix Isolation Infrared Study. *J. Phys. Chem. A* **2010**, *114*, 5919–5927.
- (14) Boeckx, B.; Maes, G. The conformational behavior and H-bond structure of asparagine: A theoretical and experimental matrix-isolation FT-IR study. *Biophys. Chem.* **2012**, *165–166*, 62–73.
- (15) Boeckx, B.; Nelissen, W.; Maes, G. Potential Energy Surface and Matrix Isolation FT-IR Study of Isoleucine. *J. Phys. Chem. A* **2012**, *116*, 3247–3258.
- (16) Boeckx, B.; Maes, G. Experimental and Theoretical Observation of Different Intramolecular H-bonds in Lysine Conformations. *J. Phys. Chem. B* **2012**, *116*, 12441–12449.
- (17) Kaczor, A.; Reva, I. D.; Proniewicz, L. M.; Fausto, R. Matrix-Isolated Monomeric Tryptophan: Electrostatic Interactions as Non-trivial Factors Stabilizing Conformers. *J. Phys. Chem. A* **2007**, *111*, 2957–2965.
- (18) Jarmelo, S.; Fausto, R. Entropy effects in conformational distribution and conformationally dependent UV-induced photolysis of serine monomer isolated in solid argon. *J. Mol. Struct.* **2006**, *786*, 175–181.
- (19) Ramaekers, R.; Pajak, J.; Rospenk, M.; Maes, G. Matrix-isolation FT-IR spectroscopic study and theoretical DFT(B3LYP)/6-31++G** calculations of the vibrational and conformational properties of tyrosine. *Spectrochim. Acta A* **2005**, *61*, 1347–1356.
- (20) Lambie, B.; Ramaekers, R.; Maes, G. Conformational Behavior of Serine: An Experimental Matrix-Isolation FT-IR and Theoretical DFT(B3LYP)/6-31++G** Study. *J. Phys. Chem. A* **2004**, *108*, 10426–10433.
- (21) Stepanian, S. G.; Reva, I. D.; Radchenko, E. D.; Adamowicz, L. Combined Matrix-Isolation Infrared and Theoretical DFT and ab Initio Study of the Nonionized Valine Conformers. *J. Phys. Chem. A* **1999**, *103*, 4404–4412.
- (22) Stepanian, S. G.; Reva, I. D.; Radchenko, E. D.; Adamowicz, L. Conformers of Nonionized Proline. Matrix-Isolation Infrared and Post-Hartree-Fock ab Initio Study. *J. Phys. Chem. A* **2001**, *105*, 10664–10672.
- (23) Cappelli, C.; Monti, S.; Rizzo, A. Effect of the Environment on Vibrational Infrared and Circular Dichroism Spectra of (S)-Proline. *Int. J. Quantum Chem.* **2005**, *104*, 744–757.
- (24) Jalkanen, K. J.; Degtyarenko, I. M.; Nieminen, R. M.; Cao, X.; Nafie, L. A.; Zhu, F.; Barron, L. D. Role of hydration in determining the structure and vibrational spectra of L-alanine and N-acetyl L-alanine N'-methylamide in aqueous solution: A combined theoretical and experimental approach. *Theor. Chem. Acc.* **2008**, *119*, 191–210.
- (25) Jalkanen, K. J.; Jürgensen, V. W.; Claussen, A.; Rahim, A.; Jensen, G. M.; Wade, R. C.; Nardi, F.; Jung, C.; Degtyarenko, I. M.; Nieminen, R. M.; Herrmann, F.; Knapp-Mohammady, M.; Niehaus, T. A.; Friman, K.; Suhai, S. Use of Vibrational Spectroscopy to Study Protein and DNA Structure, Hydration, and Binding of Biomolecules: A Combined Theoretical and Experimental Approach. *Int. J. Quantum Chem.* **2006**, *106*, 1160–1198.
- (26) Zhu, P.; Yang, G.; Poopari, M. R.; Bie, Z.; Xu, Y. Conformations of Serine in Aqueous Solutions as Revealed by Vibrational Circular Dichroism. *ChemPhysChem* **2012**, *13*, 1272–1281.
- (27) Poopari, M. R.; Zhu, P.; Dezhahang, Z.; Xu, Y. Vibrational absorption and vibrational circular dichroism spectra of leucine in water under different pH conditions: Hydrogen-bonding interactions with water. *J. Chem. Phys.* **2012**, *137*, 194308.
- (28) Poopari, M. R.; Dezhahang, Z.; Yang, G.; Xu, Y. Conformational distributions of N-acetyl-L-cysteine in aqueous solutions: A combined implicit and explicit solvation treatment of VA and VCD spectra. *ChemPhysChem* **2012**, *13*, 2310–21.
- (29) Kamiński, M.; Kudelski, A.; Pecul, M. Vibrational Optical Activity of Cysteine in Aqueous Solution: A Comparison of Theoretical and Experimental Spectra. *J. Phys. Chem. B* **2012**, *116*, 4976–4990.
- (30) Hopmann, K. H.; Ruud, K.; Pecul, M.; Kudelski, A.; Dračinský, A.; Bouř, P. Explicit versus Implicit Solvent Modeling of Raman Optical Activity Spectra. *J. Phys. Chem. B* **2011**, *115*, 4128–4137.
- (31) Schlosser, D. W.; Devlin, F.; Jalkanen, K.; Stephens, P. J. Vibrational circular dichroism of matrix-isolated molecules. *Chem. Phys. Lett.* **1982**, *88*, 286–291.
- (32) Henderson, D. O.; Polavarapu, P. Fourier transform infrared vibrational circular dichroism of matrix-isolated molecules. *J. Am. Chem. Soc.* **1986**, *108*, 7110–7111.
- (33) Tarczay, G.; Magyarfalvi, G.; Vass, E. Towards the determination of the absolute configuration of complex molecular systems: Matrix isolation vibrational circular dichroism study of (R)-2-amino-1-propanol. *Angew. Chem., Int. Ed.* **2006**, *45*, 1775–1777.
- (34) Merten, C.; Xu, Y. Chirality transfer in a methyl lactate-ammonia complex observed by matrix-isolation vibrational circular dichroism spectroscopy. *Angew. Chem., Int. Ed.* **2013**, *52*, 2073–2076.
- (35) Yang, G.; Xu, Y. Vibrational circular dichroism spectroscopy of chiral molecules. *Top. Curr. Chem.* **2011**, *298*, 189–236.
- (36) Pecul, M. *Modeling of Solvation Effects on Chiroptical Spectra*. In *Comprehensive Chiroptical Spectroscopy, Vol. 1: Instrumentation, Methodologies, and Theoretical Simulations*; Berova, N., Polavarapu, P. L., Nakanishi, K., Woody, R. W., Eds.; John Wiley & Sons, Inc.: Hoboken, NJ, 2012; pp 729–745.
- (37) *Solvent Effects on Natural Optical Activity in Continuum Solvation Models in Chemical Physics: From Theory to Applications*; Mennucci, B., Cammi, R., Eds.; Wiley-VCH: Weinheim, Germany, 2007.
- (38) Pecul, M.; Ruud, K. *Solvent Effect on Natural Optical Activity*. In: *Solvent Effects on Natural Optical Activity in Continuum Solvation Models in Chemical Physics: From Theory to Applications*; Mennucci, B., Cammi, R., Eds.; Wiley-VCH: Weinheim, Germany; , 2007; pp 206–219.
- (39) Dobrowolski, J. Cz.; Lipiński, P. F. J.; Rode, J. E.; Sadlej, J. α -Amino Acids in Water: A Review on VCD and ROA Spectra. In *Optical Spectroscopy and Computational Methods in Biology and Medicine*; Baranska, M., Ed.; Challenges and Advances in Computational Chemistry and Physics; Springer Science and Business Media: Dordrecht, The Netherlands; 2014; Vol. 14.
- (40) Brosnan, J. T.; Brosnan, M. E.; Bertolo, R. F. P.; Brunton, J. A. Methionine: A metabolically unique amino acid. *Livestock Science* **2007**, *112*, 2–7.
- (41) Levine, R. L.; Mosoni, L.; Berlett, B. S.; Stadtman, E. R. Methionine residues as endogenous antioxidants in proteins. *Proc. Natl. Acad. Sci. U.S.A.* **1996**, *93*, 15036–15040.
- (42) Jamróz, M. H.; Rode, J. E.; Ostrowski, S.; Lipiński, P. F. J.; Dobrowolski, J. Cz. Chirality Measures of α -Amino Acids. *J. Chem. Inform. Model* **2012**, *52*, 1462–1479.
- (43) Cao, X.; Fisher, G. Conformational and Infrared Spectral Studies of L-Methionine and Its N-Deuterated Isotopomer as Isolated Zwitterions. *J. Phys. Chem. A* **2002**, *106*, 41–50.
- (44) Hernandez, B.; Pflüger, F.; Adenier, A.; Kruglik, S. G.; Ghomi, M. Side chain flexibility and protonation states of sulfur atom containing amino acids. *Phys. Chem. Chem. Phys.* **2011**, *13*, 17284–17294.
- (45) Mary, M. B.; Umadevi, M.; Pandiarajan, S.; Ramakrishnan, V. Vibrational spectral studies of L-methionine L-methioninium perchlorate monohydrate. *Spectrochim. Acta, Part A* **2004**, *60*, 2643–2651.
- (46) Yamanobe-Hada, M.; Ito, A.; Shindo, H. J. Study of spontaneous cleavage and change in surface structure of DL-methionine crystals. *Cryst. Growth* **2005**, *275*, e1739–e1743.
- (47) Ramachandran, E.; Natarajan, S. Gel growth and characterization of β -DL-methionine. *Cryst. Res. Technol.* **2006**, *41*, 411–415.
- (48) Koleva, B. B. Solid-state linear-polarized IR-spectroscopic characterization of L-methionine. *Vib. Spectr.* **2007**, *44*, 30–35.
- (49) Lima, J. A., Jr.; Freire, P. T. C.; Melo, F. E. A.; Lemos, V.; Mendes Filho, J.; Pizani, P. S. High pressure Raman spectra of L-methionine crystal. *J. Raman Spectrosc.* **2008**, *39*, 1356–1363.
- (50) Nafie, L. A.; Oboodi, M. R.; Freedman, T. B. Vibrational Circular Dichroism in Amino Acids and Peptides. 8. A Chirality Rule for the Methine C $^*_\alpha$ -H Stretching Mode. *J. Am. Chem. Soc.* **1983**, *105*, 7449–7450.
- (51) Oboodi, M. R.; Lal, B. B.; Young, D. A.; Freedman, T. B.; Nafie, L. A. Vibrational Circular Dichroism in Amino Acids and Peptides. 9.

Carbon-Hydrogen Stretching Spectra of the Amino Acids and Selected Transition Metal Complexes. *J. Am. Chem. Soc.* **1985**, *107*, 1547–1556.

(52) Shanmugam, G.; Polavarapu, P. L. Film Techniques for Vibrational Circular Dichroism Measurements. *Appl. Spectrosc.* **2005**, *59*, 673–681.

(53) Zhang, P.; Polavarapu, P. L. Vibrational circular dichroism of matrix-assisted amino acid films in the mid-infrared region. *Appl. Spectrosc.* **2006**, *60*, 378–385.

(54) Zhang, P. *Chiral Separations and Chiroptical Spectroscopic Studies*. PhD Thesis, Graduate School of Vanderbilt University, Nashville, TN, 2006.

(55) Ji, Z.; Santamaria, R.; Garzón, I. L. Vibrational Circular Dichroism and IR Absorption Spectra of Amino Acids: A Density Functional Study. *J. Phys. Chem. A* **2010**, *114*, 3591–3601.

(56) Becke, A. D. Density-functional thermochemistry. III. The role of exact exchange. *J. Chem. Phys.* **1993**, *98*, 5648–5652.

(57) Burke, K.; Perdew, J. P.; Wang, Y. *Electronic Density Functional Theory: Recent Progress and New Directions*; Dobson, J. F., Vignale, G., Das, M. P., Eds.; Plenum, 1998.

(58) Møller, C.; Plesset, M. S. Note on an Approximation Treatment for Many-Electron Systems. *Phys. Rev.* **1934**, *46*, 618–622.

(59) Boeckx, B.; Ramaekers, R.; Maes, G. A theoretical and matrix-isolation FT-IR investigation of the conformational landscape of *N*-acetylcysteine. *J. Mol. Spectrosc.* **2010**, *261*, 73–81.

(60) Dunning, T. H., Jr. Gaussian basis sets for use in correlated molecular calculations. I. The atoms boron through neon and hydrogen. *J. Chem. Phys.* **1989**, *90*, 1007–1023.

(61) Kendall, R. A.; Dunning, T. H.; Harrison, R. J. Electron affinities of the first-row atoms revisited. Systematic basis sets and wave functions. *J. Chem. Phys.* **1992**, *96*, 6796–6806.

(62) Spartan '08; Wavefunction, Inc.: Irvine, CA; www.wavefun.com.

(63) Mennucci, B. Polarizable continuum model. *Wiley Interdiscip. Rev.: Comput. Mol. Sci.* **2012**, *2*, 386–404.

(64) Scalmani, G.; Frisch, M. J. Continuous surface charge polarizable continuum models of solvation. I. General formalism. *J. Chem. Phys.* **2010**, *132*, 114110.

(65) Frisch, M. J.; Trucks, G. W.; Schlegel, H. B.; Scuseria, G. E.; Robb, M. A.; Cheeseman, J. R.; Scalmani, G.; Barone, V.; Mennucci, B.; Petersson, G. A. et al. *Gaussian 09*, revision A.1; Gaussian, Inc.: Wallingford, CT, 2009.

(66) Lambie, B.; Ramaekers, R.; Maes, G. On the contribution of intramolecular H-bonding entropy to the conformational stability of alanine conformations. *Spectrochim. Acta, Part A* **2003**, *59*, 1387–1397.

(67) Linder, R.; Seefeld, K.; Vavra, A.; Kleinermanns, K. Gas phase infrared spectra of nonaromatic amino acids. *Chem. Phys. Lett.* **2008**, *453*, 1–6.

(68) Dalhus, B.; Görbitz, C. H. Crystal Structures of Hydrophobic Amino Acids I. Redeterminations of L-Methionine and L-Valine at 120 K. *Acta Chem. Scand.* **1996**, *50*, 544–548.